

# On the Best Integer Equivariant Estimator for Low-cost Single-frequency Multi-GNSS RTK Positioning

ROBERT ODOLINSKI

National School of Surveying, University of Otago, Dunedin, New Zealand

PETER J.G. TEUNISSEN

GNSS Research Centre, Curtin University, Perth, Australia and

Mathematical Geodesy and Positioning, Delft University of Technology, Delft, the Netherlands

## BIOGRAPHY

Robert is currently a Senior Lecturer at the School of Surveying, University of Otago. Robert is a member of the International Association of Geodesy (IAG) ICCT Joint Study Group 'Multi-GNSS Theory and Algorithms', and is a co-chair of the IAG working groups on 'Reliability of low-cost & Android GNSS in navigation and geosciences' and 'Ambiguity resolution for low-cost GNSS receiver positioning', respectively.

Peter J.G. Teunissen is currently a Professor of geodesy and navigation, and the Head of the GNSS Research Centre at Curtin University. He is also with Department of Geoscience and Remote Sensing, Delft University, Delft, The Netherlands. His current research interests include multiple GNSSs and the modeling of next-generation GNSS for high-precision positioning, navigation, and timing applications.

## ABSTRACT

Carrier phase integer ambiguity resolution with a high success rate is the key to precise Global Navigation Satellite System (GNSS) positioning. When the success rate is too low the user will normally prefer the float solution, whereas the alternative can be to use the Best Integer Equivariant (BIE) estimator. Low-cost receiver real-time kinematic (RTK) precise positioning has become possible through combining signals from several GNSSs, such as BDS, Galileo, QZSS, and GPS. In this contribution we will use single-frequency (SF) low-cost receiver multi-GNSS data to compare the performance of the BIE estimator and the standard method of Integer Least Squares (ILS). The GNSS data is evaluated in Dunedin, New Zealand, with short baselines so that the relative atmospheric delays can be neglected. We show, with real multi-GNSS data and when the success rate is at low to medium levels, that the positioning performance of the BIE estimator will resemble or be better than that of the float solution, and always be better in the minimum mean squared error (MMSE) sense than the ILS fixed solutions. Whereas for very high success rates we get a BIE performance similar to that of the ILS estimator and much better than the float solution.

**Keywords:** Best Integer Equivariant (BIE) estimation, Integer Least Squares (ILS) estimation, Low-cost Receiver, Single-frequency Real Time Kinematic (RTK) positioning, Multi-GNSS

## INTRODUCTION

Carrier-phase integer ambiguity resolution is the key to high precision Global Navigation Satellite System (GNSS) real-time kinematic (RTK) positioning. The combination of several GNSSs like the Chinese BeiDou Navigation Satellite System (BDS), European Galileo, Japanese Quasi-Zenith Satellite System (QZSS) and American Global Positioning System (GPS) has also made low-cost receiver [1–4] and smartphone precise positioning possible [5–9].

The method to obtain RTK derived positions is to fix the full or partial [10–13] integer vector when the corresponding ambiguity success rate is very high [14]. On the other hand when the success rate is low, one usually opts for the float

solution.

The alternative can be to use Teunissen's Best Integer Equivariant (BIE) estimator. As is shown in [15], the BIE-estimator is optimal in the minimum mean squared error (MMSE) sense. It therefore outperforms the float and fixed Integer Least Squares (ILS) solutions in this sense [15–17]. As the BIE-estimator is a weighted sum over the space of integers, it also has the advantage that no integer validation test is needed. However, as a sum over the whole space of integers is impractical, [18] has shown how the integer-summation can be taken over a finite integer set, while still maintaining the important property of integer-equivariance. [16, 17, 19] used simulation to look at the distributional properties and positioning performance of the BIE estimator when compared to the float and ILS fixed counterparts.

In this contribution we will look at the BIE performance using real multi-GNSS data from single-frequency (SF) low-cost RTK receivers. With 'low-cost' we refer to a combined cost for a multi-GNSS receiver and antenna of at most a few hundred USDs. First we define our functional model and show how the standard ILS ambiguity and baseline solution is derived. We also describe the BIE estimator and its approximation. This is then followed by a brief description of the GNSS baseline employed. BIE results for short baseline multi-GNSS data is then depicted and compared to that of ILS and the ambiguity-float counterparts. With short baseline we refer to the case where the ionospheric and tropospheric delays can be assumed absent. Finally we end up with a summary and conclusions.

## FUNCTIONAL RTK MODEL

In the following system of observation equations we assume that we have access to SF and double-differenced (DD) code and phase data of GPS, BDS, Galileo, and QZSS. When we refer to BDS we refer to the BDS-2 regional system [20, 21] and not the global BDS-3 constellation [22]. Satellite orbits and clocks are obtained through the broadcast ephemeris, and we omit time stamps for brevity. We make use of a common reference satellite on the overlapping frequencies (L1 GPS, E1 Galileo and L1 QZSS) between the systems to maximize the model strength [7, 23, 24]. The linearized system of DD observation equations read,

$$E(y) = Aa + Bb, \quad a \in \mathbb{Z}^n, b \in \mathbb{R}^p \quad (1)$$

where  $E(\cdot)$  is the expectation operator,  $y$  the vector of code and phase observations of size  $m$ ,  $a$  is the  $n$  vector of unknown integer ambiguities, and  $b$  the  $p$  vector of real-valued baseline components like the coordinates. For sufficiently long baselines, it also includes ionospheric and tropospheric delays. The design matrices  $A$  and  $B$  are of size  $m \times n$  and  $m \times p$ , respectively, and are assumed to be of full rank.

## INTEGER LEAST SQUARES ESTIMATION

The GNSS model (1) is solved in the following three-step procedure [14].

### The float solution

Firstly we assume the ambiguities in (1) to be real-valued parameters  $a \in \mathbb{R}^n$  and perform a LS adjustment [25], so as to obtain the so called 'float solution' of the ambiguities and baseline components, denoted with a 'hat', as,

$$\begin{bmatrix} \hat{a} \\ \hat{b} \end{bmatrix}, \quad \begin{bmatrix} Q_{\hat{a}\hat{a}} & Q_{\hat{a}\hat{b}} \\ Q_{\hat{b}\hat{a}} & Q_{\hat{b}\hat{b}} \end{bmatrix} \quad (2)$$

where  $Q_{\hat{b}\hat{a}}^T = Q_{\hat{a}\hat{b}}$  are the float covariance matrices and  $Q_{\hat{b}\hat{b}}, Q_{\hat{a}\hat{a}}$  the baseline and ambiguity variance-covariance (vc) matrices, respectively. The second step is to solve the ILS problem making use of the float ambiguities  $\hat{a} \in \mathbb{R}^n$  in (2) and search for its corresponding integer solution  $a \in \mathbb{Z}^n$ .

### Integer ambiguity estimation and LAMBDA

This step constitutes of decorrelating the ambiguities through the LAMBDA method  $\hat{z} = Z^T \hat{a}$  so as to obtain an almost diagonal vc-matrix  $Q_{\hat{z}\hat{z}} = Z^T Q_{\hat{a}\hat{a}} Z$ . We then find the *single* integer candidate vector through an integer search that minimizes the weighted squared norm,

$$\arg \min_{z \in \mathbb{Z}^n} \|\hat{z} - z\|_{Q_{\hat{z}\hat{z}}}^2 \quad (3)$$

where  $\|.\|_{Q_{\hat{z}\hat{z}}}^2 = (.)^T Q_{\hat{z}\hat{z}}^{-1} (.)$ . The search is conducted by testing potential grid points inside the ellipsoid, so called integer candidates. The integer points inside the ellipsoid that can be derived as the minimum value of the squared norm  $\|\hat{z} - z\|_{Q_{\hat{z}\hat{z}}}^2$  is the optimal integer solution denoted with 'check',  $\check{z}$ . We refer to this single integer vector solution as the ILS solution, which is optimal in the sense that it gives the highest possible success rates of all integer estimators [26, 27]. Once we have the ILS solution  $\check{z}$  we are in the position for the third and final step, which is to compute our fixed baseline solution.

### Fixed solution

In the third step we compute the fixed baseline solution. We transform  $\check{a} = Z^{-T} \check{z}$  and then compute the fixed baseline solution  $\check{b}$  as,

$$\check{b} = \hat{b} - Q_{\hat{b}\hat{a}} Q_{\hat{a}\hat{a}}^{-1} (\hat{a} - \check{a}) \quad (4)$$

which, when  $\check{a}$  is treated deterministically, has the corresponding vc-matrix,

$$Q_{\check{b}\check{b}} = Q_{\hat{b}\hat{b}} - Q_{\hat{b}\hat{a}} Q_{\hat{a}\hat{a}}^{-1} Q_{\hat{a}\hat{b}} \quad (5)$$

One can infer from (5) that the fixed baseline precision can be radically improved by the subtraction of  $Q_{\hat{b}\hat{a}} Q_{\hat{a}\hat{a}}^{-1} Q_{\hat{a}\hat{b}}$  provided that the uncertainty in  $\check{a}$  may be neglected. This since the float baseline precision in  $Q_{\hat{b}\hat{b}}$  is dominated by the relatively poor code precision for short time spans, while  $Q_{\hat{a}\hat{a}}$  is based on the very precise phase data, and thus  $Q_{\check{b}\check{b}}$  will become very precise as well (provided also that a high correlation between the ambiguities and the baseline exists). However, this baseline improvement will only happen if the integer ambiguities  $\check{a}$  have been solved with a sufficiently high success rate close to one.

### BEST INTEGER EQUIVARIANT ESTIMATION

On the other hand when the success rate is too low, the user will normally prefer the float  $\hat{b}$  in (2) rather than the fixed solution  $\check{b}$  in (4). The alternative in such cases can be to use the BIE estimator [15] to solve for the ambiguities. Assuming normally distributed data, the BIE-estimator of the ambiguities, denoted with 'overline', is then given as,

$$\bar{a} = \sum_{z \in \mathbb{Z}^n} z \frac{\exp\left(-\frac{1}{2} \|\hat{a} - z\|_{Q_{\hat{a}\hat{a}}}^2\right)}{\sum_{z \in \mathbb{Z}^n} \exp\left(-\frac{1}{2} \|\hat{a} - z\|_{Q_{\hat{a}\hat{a}}}^2\right)} \quad (6)$$

where  $\bar{a}$  is defined by an infinite weighted sum over the whole space of integers. The BIE baseline solution can then be derived as,

$$\bar{b} = \hat{b} - Q_{\hat{b}\hat{a}} Q_{\hat{a}}^{-1} (\hat{a} - \bar{a}) \quad (7)$$

where the ILS solution  $\check{a}$  in (4) has been replaced by the BIE solution  $\bar{a}$  computed in (6). Since the BIE solution in (6) involves an infinite weighted sum, which is computationally impractical, [18] has shown how one can make use of a finite integer set  $\Theta_{\hat{a}}^\lambda$ , while still maintaining the property of integer-equivariance,

$$\bar{a}^\lambda = \sum_{z \in \Theta_{\hat{a}}^\lambda} z \frac{\exp\left(-\frac{1}{2} \|\hat{a} - z\|_{Q_{\hat{a}\hat{a}}}^2\right)}{\sum_{z \in \Theta_{\hat{a}}^\lambda} \exp\left(-\frac{1}{2} \|\hat{a} - z\|_{Q_{\hat{a}\hat{a}}}^2\right)} \quad (8)$$

where  $z \in \mathbb{Z}^n$  in (6) has been replaced by  $z \in \Theta_{\hat{a}}^\lambda$  in (8). The integers that reside in the set  $\Theta_{\hat{a}}^\lambda$  depends then on the ellipsoidal region around the float solution  $\hat{a}$  with its radius defined in the metric of  $Q_{\hat{a}\hat{a}}$ , which can be defined as follows [18],

$$\|\hat{a} - z\|_{Q_{\hat{a}\hat{a}}}^2 < \lambda^2 \quad (9)$$

where the threshold  $\lambda^2$  can be determined from a central Chi-squared distribution  $\chi^2$  with  $n$  degrees of freedom and a small significance level  $\alpha$ . In this article we choose  $\alpha = 10^{-16}$ , which is the same setting that maximized the number of integer candidates in [28] based on Monte-Carlo simulations. We remark that to find the integer vectors that lie within the set (9) in an efficient manner, one would first make use of the Z-transformation of the LAMBDA method such that the ellipsoidal search space becomes more spherical.

It was demonstrated in [15] that the BIE estimator is unbiased and that it minimizes the Mean Squared Errors (MSEs), and the positioning precision of the BIE baseline estimator (7) is thus at least as good as the ILS (4) and float solution (2), respectively, i.e. we have:

$$\begin{aligned} D(\bar{b}) &\leq D(\check{b}) \\ D(\bar{b}) &\leq D(\hat{b}) \end{aligned} \quad (10)$$

where  $D(\cdot)$  is the dispersion operator. Note that BIE becomes similar to the ILS solution when the success rate is very high, and similar to the float solution when the success rate is very low [15]. In the following section we will evaluate how this hold true for the BIE approximation in (8) and real SF multi-GNSS low-cost receiver data collected in Dunedin, NZ.

### BIE FOR SINGLE-EPOCH LOW-COST SF MULTI-GNSS RTK POSITIONING

In order to analyze the BIE RTK positioning performance, we will use 48 h (30 s measurement interval) of u-blox M8T receiver and patch antenna data using SF GPS+Galileo+QZSS+BDS in Dunedin, NZ and a 670 m baseline. Hence we are able to neglect the relative atmospheric delays, which we here refer to as the 'ionosphere-fixed' model. The number of satellites of this data is depicted in Figure 1, where an elevation cut-off angle of  $20^\circ$  is mainly used to avoid low-elevation multipath. The stochastic model settings are depicted in Table 1, where the undifferenced and zenith-referenced standard deviations (STDs) were obtained through least squares variance component estimation (LS-VCE) and independent data similar to [7]. An exponential elevation weighting function was also used [29].

Table 1: Undifferenced and zenith-referenced STDs for code ( $\hat{\sigma}_{p_j}$ ) and phase ( $\hat{\sigma}_{\phi_j}$ ) for a SF L1+E1+L1+B1 GPS+Galileo+QZSS+BDS model, with an elevation cut-off angle of  $20^\circ$  over 48 h (30 s) of data collected in Dunedin, NZ at 5 Jan, 2018 from 05:00 (hh:mm) UTC

	$\hat{\sigma}_{p_j}$ [cm]	$\hat{\sigma}_{\phi_j}$ [mm]
L1 GPS	45	2
E1 Galileo	41	2
L1 QZSS	48	2
B1 BDS	58	2

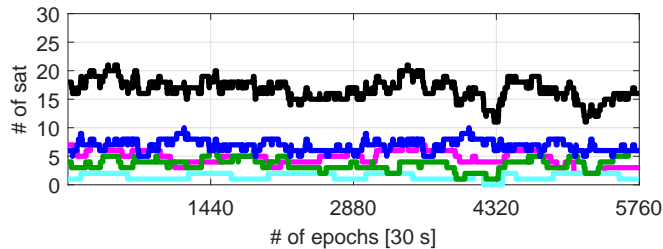


Figure 1: Number of satellites for SF GPS+Galileo+QZSS+BDS with an elevation cut-off angle of  $20^\circ$  for the multi-GNSS data collected in Dunedin, NZ (Table 1). The *black line* corresponds to a combined 4-system model, *blue line* GPS, *green line* Galileo, *cyan line* QZSS, and *magenta line* BDS

Figure 2 depicts the single-epoch estimated horizontal (local North and East) positioning errors, based on the 48 h of multi-GNSS data and when compared to very precise benchmark coordinates. The BIE performance of the local Up component behaves in a similar manner and is thus not shown here for brevity. The benchmark coordinates were obtained by averaging all single-epoch estimated coordinates derived while assuming the ambiguities to be time-constant over the whole observation time span and combining all four systems (c.f. Figure 1), so as to maximize the model strength with a 100% ILS success rate (SR). The ambiguity-float, ILS and BIE SF ionosphere-fixed positioning errors are denoted as black, magenta and green dots, respectively. We make use of a zoom-in window to depict the two-order of magnitude improvement when going from float to correctly fixed ILS solutions. To vary the ILS SRs we look at different positioning models, with top left to bottom right panels depicting the results for an L1 GPS model and an elevation cut-off angle of  $20^\circ$ , but we remove four random GPS satellites here to make the model weaker. This follows by L1 GPS ( $20^\circ$  cut-off without removing satellites), L1 GPS (cut-off  $10^\circ$ ), L1+E1 GPS+Galileo (cut-off  $20^\circ$ ), L1+E1+L1 GPS+Galileo+QZSS (cut-off  $20^\circ$ ), and L1+E1+L1+B1

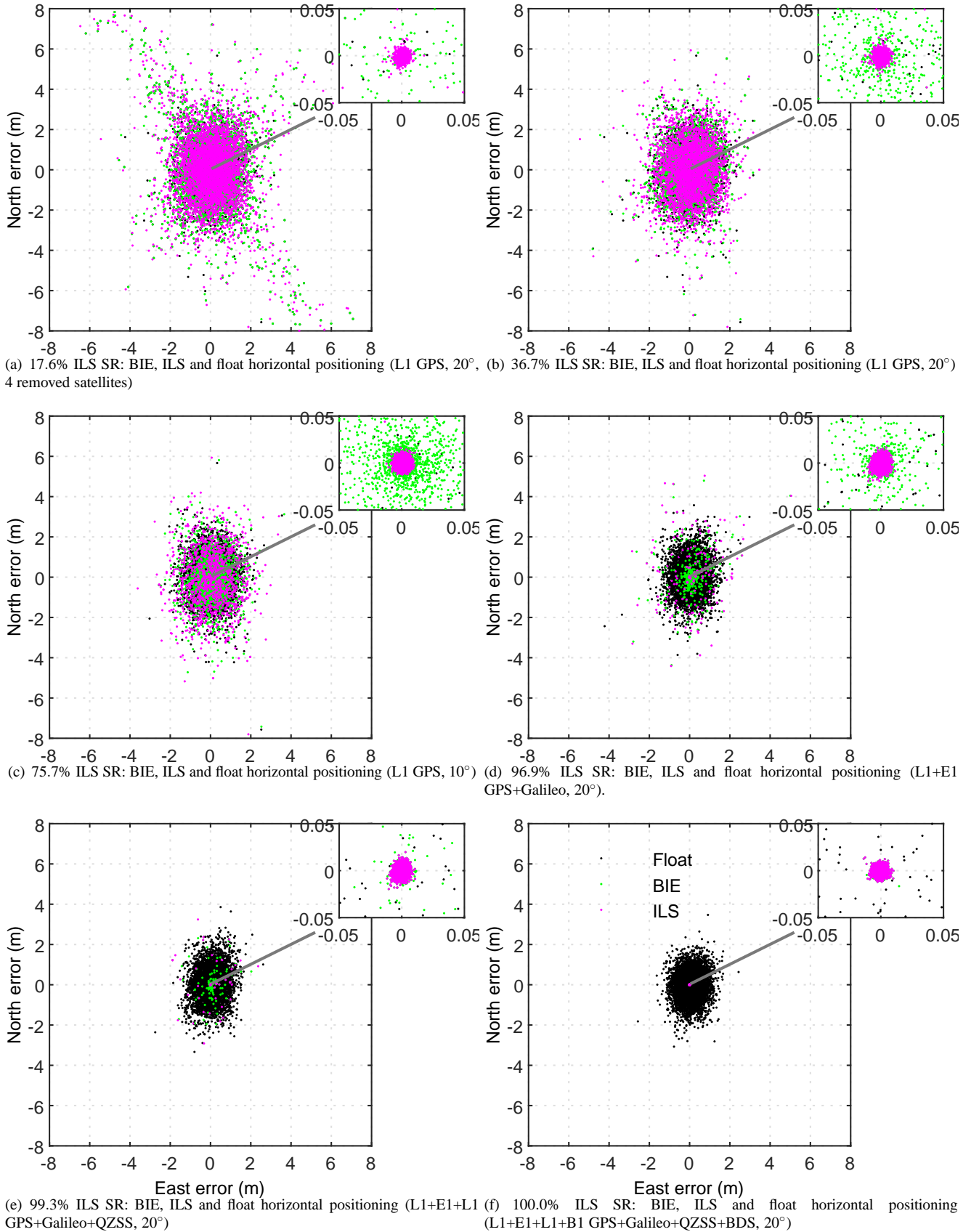


Figure 2: Horizontal (North/East) scatter of the multi-GNSS data derived BIE (green dots), ILS (magenta dots), and ambiguity-float (black dots) ionosphere-fixed SF RTK positioning for a 670 m baseline in Dunedin, NZ, based on two days of data (48 h, 30 s measurement interval) and ublox EVK-M8T+patch antennas. The corresponding histograms are depicted in Figure 3. Finally the zoom-in window is used to depict the two-order of magnitude improvement when going from float to ILS fixed solutions.

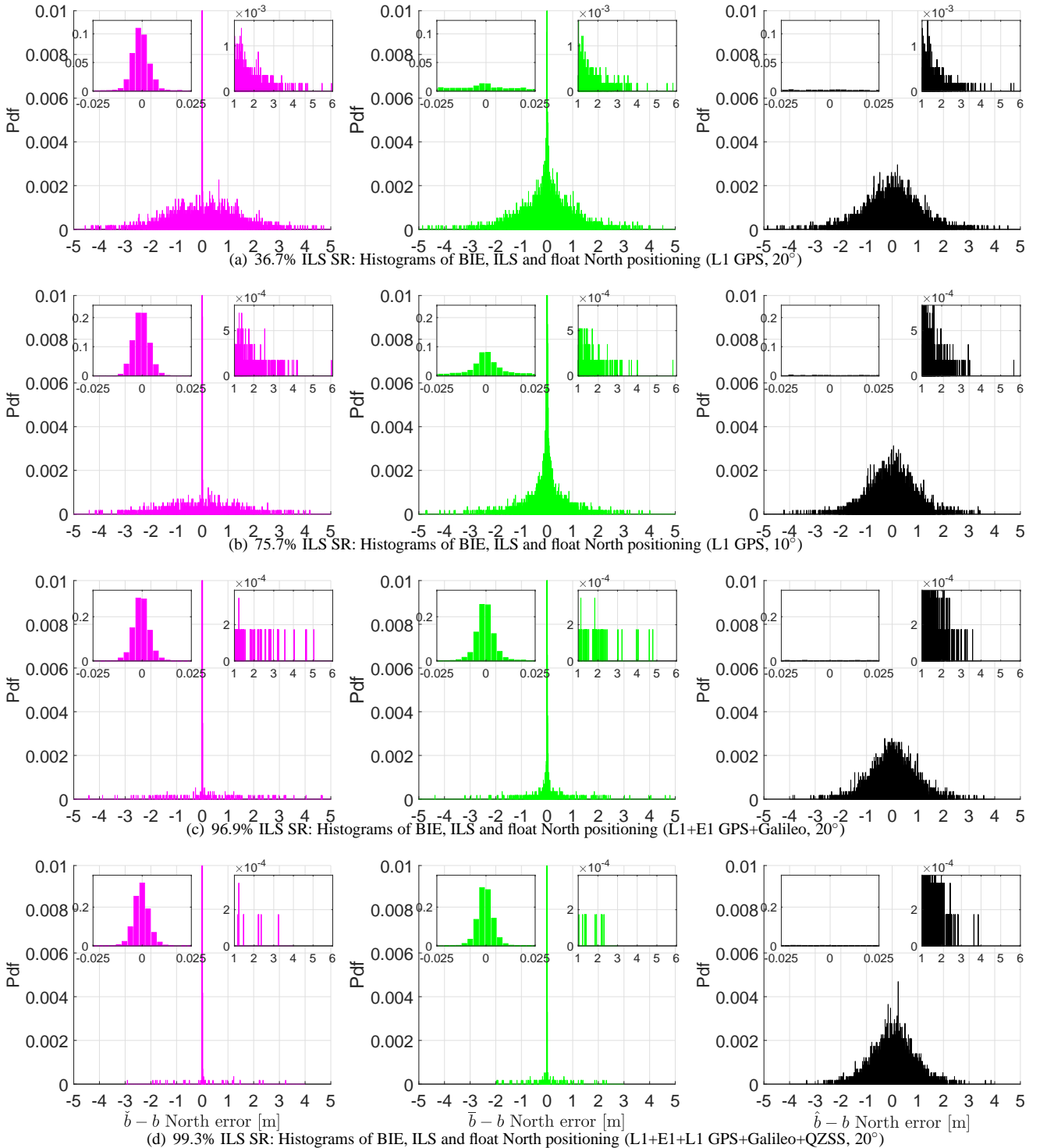


Figure 3: Example histograms (bin size of 3 mm) of the multi-GNSS data derived North positioning errors in Figure 2 of the BIE (*green bars*), ILS (*magenta bars*), and ambiguity-float (*black bars*) solutions. The East and Up positioning histograms behave in a similar manner and are thus not shown for brevity. The zoom-in windows depicted for the ILS solutions are examples of the PDF of North errors between  $-0.025$  and  $0.025$  m and  $1.0$  to  $6.0$  m, respectively. Note that the y-axis for the zoom-in windows are generally different between each row, so that a direct comparison can be made between ILS, BIE and ambiguity-float solutions for each model strength

GPS+Galileo+QZSS+BDS (cut-off 20°), respectively. The ILS SR was computed by comparing the single-epoch estimated ambiguities to a set of reference ambiguities. These reference ambiguities were obtained by using a four-system model, with ambiguities again kept time-constant over the entire time span, while the precise baseline and the satellite coordinates, as obtained from the broadcast ephemerides, are used so as to fix a known range (referred to as the 'geometry-fixed' model).

Figure 3 shows a selection of the corresponding histograms for the North positioning errors, where the East and Up component behave in a similar manner and are thus not shown for brevity. In this figure the BIE solutions are shown as green, ILS as magenta and float as black bars. Zoom-in windows are given for North errors between  $-0.025$  to  $0.025$  m and  $1.0$  to  $6.0$  m, respectively, so as to show that the BIE estimator overall has a smaller amount of large positioning errors than both ILS and the float solutions, and that its positioning performance resembles that of ILS and outperforms the float solutions for high ILS SRs.

Figure 2 shows that for low ILS SRs, at the top row, the BIE solutions (green dots) resemble the float solutions (black dots underneath or near the green dots), whereas when the model gets stronger at the middle and bottom panels the BIE solutions outperform the ambiguity-float counterparts. This is confirmed by inspecting the corresponding histograms in Figure 3. Figure 3 shows further that there are several ILS solutions that are further away from zero meters than BIE. For instance, for the SF GPS+Galileo model (ILS SR of 96.9%) at the third row and in the zoom-in window we can see several ILS North positioning errors above 2.5 m, whereas the number of such solutions are fewer for BIE.

To further illustrate that BIE has fewer large positioning errors than ILS, Figure 4 depicts the cumulative distribution functions (CDFs) of the 3D BIE, ILS and ambiguity-float positioning results with a 95% confidence interval (CI) as green, magenta, black and dashed black line, respectively. We can see in top left row of Figure 4 when we have an ILS SR of 36.7%, that the BIE solutions start to become better than ILS for a CDF of about 48% and better than the float solutions until around 98% where they become similar (and BIE still remains better than ILS). Hence the corresponding 95% 3D positioning CI of BIE is smaller than both ILS and the float solutions. We can see similar results for the ILS SR of 75.7% in the top row and right column, where one would certainly not fix the ambiguities in practice, and the 95% CI of BIE is smaller than both ILS and the float solutions. On the other hand when the ILS SR reaches 96.9%, at the left bottom row, the 95% CI is obviously smaller for ILS, but, at the same time, as shown and discussed in Figure 3, BIE then also has fewer large positioning errors. Finally for an ILS SR of 99.3% at bottom row and right column of Figure 4, BIE is always better than the float solution and similar to the ILS estimator (c.f. Figure 3).

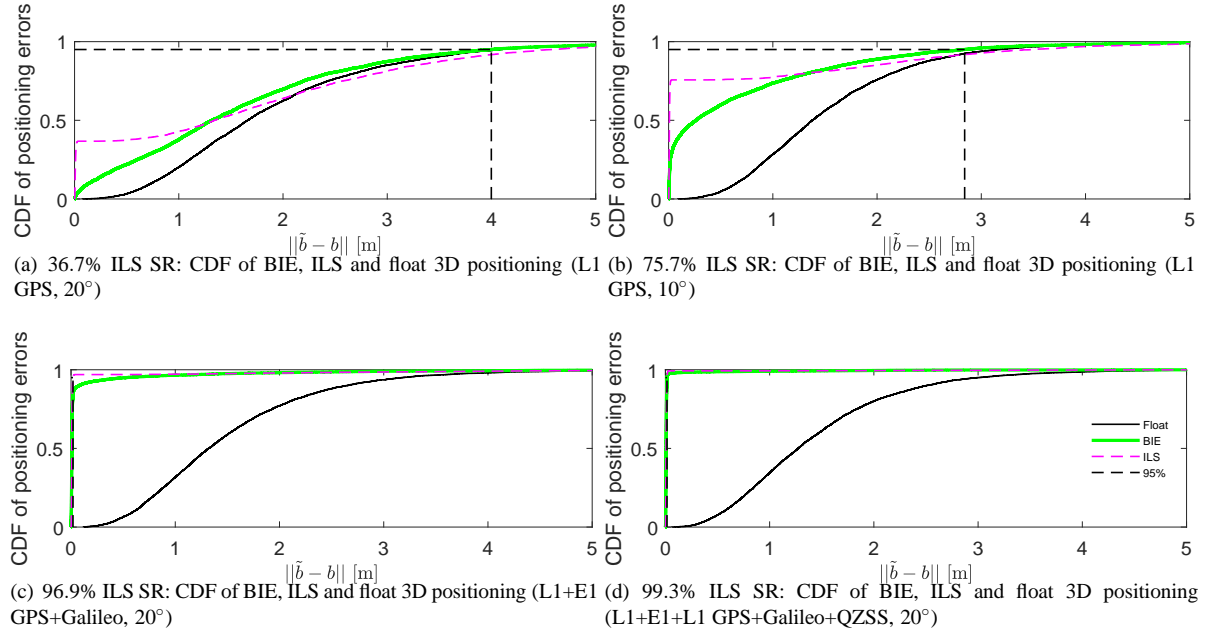


Figure 4: CDF of a selection of the BIE, ILS, ambiguity-float and ionosphere-fixed (670 m baseline, ublox+patch) SF single-epoch RTK 3D positioning errors in Figure 2.  $\tilde{b}$  are either the float  $\hat{b}$  (black line), ILS  $\check{b}$  (magenta dashed line) and BIE  $\bar{b}$  (green line) estimated 3D coordinates, respectively, and  $\|\cdot\|$  is the norm of this vector. The dashed black line corresponds to the 95% CI

Figure 5 shows the MSEs ratios of BIE as green and ILS as dashed magenta line, relative to the ambiguity-float solutions, and with the float vs float ratio given as a black line. Since the estimated positions are unbiased (c.f. Figure 3), the MSEs equal the sum of the variances of North, East and Up. Figure 5 shows that ILS has indeed a larger MSE than the float solutions for an ILS SR up to about 40%, and always larger than BIE until we reach an ILS SR of 100% (when they become similar). Finally, the MSE of BIE is always better than that of the float and ILS-fixed solutions (except for the 100% ILS SR case), which confirms (10).

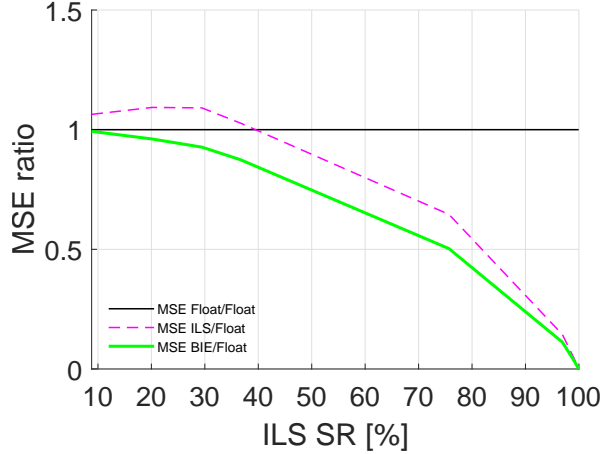


Figure 5: MSE ratios (all vs float) of the ambiguity-float and ionosphere-fixed (670 m baseline, ublox+patch) SF single-epoch RTK positioning errors in Figure 2, with BIE (*green line*), ILS (*dashed magenta line*), ambiguity-float (*black line*)

## CONCLUSIONS

In this article we evaluated the Best Integer Equivariant (BIE) estimator (6) through its approximated version (8), which was obtained by taking the integer-summation over a finite integer set that depends on the float solution and its variance matrix. The single-epoch BIE performance was compared to that of Integer Least Squares (ILS) and its ambiguity-float counterpart for short-baseline, single-frequency (SF) multi-GNSS low-cost receiver data, collected in Dunedin, NZ. With 'low-cost' we refer to a combined cost for a multi-GNSS receiver and antenna of at most a few hundred USDs. We computed single-epoch positioning errors by comparing the BIE, ILS and ambiguity-float estimated positions to very precise benchmark coordinates, and evaluated simultaneously the single-epoch ILS success rates (SRs). This was done for different combinations of L1 GPS, E1 Galileo, L1 QZSS and B1 BDS data. It was demonstrated that the BIE positioning performance resembles or is better than that of the float solution and better than ILS fixed solutions when the ILS SR is at low to medium levels, where one would not fix the ambiguities to integers in practice. Whereas for very high ILS SRs we get a BIE performance similar to that of the ILS estimator and better than the float solution.

## ACKNOWLEDGEMENTS

Kade Phillips, School of Surveying of University of Otago, collected the GNSS data. Dr Andreas Brack, GFZ Potsdam, gave valuable insights during his visit in Dunedin on the BIE estimator. The second author is the recipient of an Australian Research Council (ARC) Federation Fellowship (project number FF0883188). All this support is gratefully acknowledged.

## REFERENCES

- [1] R. Odolinski and P. J. G. Teunissen, "Single-frequency, dual-GNSS versus dual-frequency, single-GNSS: A low-cost and high-grade receivers GPS-BDS RTK analysis," *J. Geod.*, vol. 90, no. 11, pp. 1255–1278, 2016. doi:10.1007/s00190-016-0921-x.
- [2] C. Mongredien, J.-P. Doyen, M. Strom, and D. Ammann, "Centimeter-Level Positioning for UAVs and Other Mass-Market Applications," in *ION GNSS*, (Portland, Oregon), September 12-16 2016.
- [3] R. Odolinski and P. J. G. Teunissen, "Low-cost, high-precision, single-frequency GPS-BDS RTK positioning," *GPS Solut.*, vol. 21, no. 3, pp. 1315–1330, 2017. doi:10.1007/s10291-017-0613-x.

- [4] Z. Nie, F. Liu, and Y. Gao, “Real-time precise point positioning with a low-cost dual-frequency GNSS device,” *GPS Solut.*, vol. 24, no. 9, 2020. <https://doi.org/10.1007/s10291-019-0922-3>.
- [5] S. Riley, W. Lentz, and A. Clare, “On the Path to Precision - Observations with Android GNSS Observables,” in *Proc. ION GNSS*, (Portland, Oregon), 25–29 September 2017.
- [6] X. Zhang, X. Tao, F. Zhu, X. Shi, and F. Wang, “Quality assessment of GNSS observations from an Android N smartphone and positioning performance analysis using time differenced filtering approach,” *GPS Solut.*, vol. 22, no. 70, 2018. <https://doi.org/10.1007/s10291-018-0736-8>.
- [7] R. Odolinski and P. J. G. Teunissen, “An assessment of smartphone and low-cost multi-GNSS single-frequency RTK positioning for low, medium and high ionospheric disturbance periods,” *J. Geod.*, vol. 93, pp. 701–722, 2019. doi: 10.1007/s00190-018-1192-5.
- [8] J. Paziewski, R. Sieradzki, and B. Radoslaw, “Signal characterization and assessment of code GNSS positioning with low-power consumption smartphones,” *GPS Solut.*, vol. 23, no. 98, 2019. <https://doi.org/10.1007/s10291-019-0892-5>.
- [9] J. Aggrey, S. Bisnath, N. Naciri, G. Shinghal, and S. Yang, “Multi-GNSS precise point positioning with next-generation smartphone measurements,” *Journal of Spatial Science*, vol. 65, no. 1, pp. 79–98, 2020. doi: 10.1080/14498596.2019.1664944.
- [10] P. J. G. Teunissen, P. Joosten, and C. C. J. M. Tiberius, “Geometry-free ambiguity success rates in case of partial fixing,” in *Proceedings of ION ITM*, (San Diego, CA, USA), pp. 201–207, 1999.
- [11] A. Brack and C. Gunther, “Generalized integer aperture estimation for partial GNSS ambiguity fixing,” *J. Geod.*, vol. 88, no. 5, pp. 479–490, 2014.
- [12] A. Brack, “On reliable data-driven partial GNSS ambiguity resolution,” *GPS Solut.*, vol. 19, no. 4, pp. 411–422, 2015.
- [13] A. Brack, “Reliable GPS+BDS RTK positioning with partial ambiguity resolution,” *GPS Solut.*, pp. 1083–1092, 2017.
- [14] P. J. G. Teunissen, “The least squares ambiguity decorrelation adjustment: a method for fast GPS integer estimation,” *J. Geod.*, 1995. 70: 65-82.
- [15] P. J. G. Teunissen, “Theory of integer equivariant estimation with application to GNSS,” *J. Geod.*, vol. 77, pp. 402–410, 2003. doi: 10.1007/s00190-003-0344-3.
- [16] S. Verhagen and P. J. G. Teunissen, “Performance comparison of the BIE Estimator with the float and fixed GNSS ambiguity estimators,” in *A Window on the Future of Geodesy*, ser. *International Association of Geodesy Symposia*, vol. 128, pp. 428–433, Springer, Berlin Heidelberg, 2005.
- [17] A. Brack, “Partial carrier-phase integer ambiguity resolution for high accuracy GNSS positioning,” *PhD dissertation, Lehrstuhl fur Kommunikation und Navigation Technische Universitat Munchen*, 2019.
- [18] P. J. G. Teunissen, “On the computation of the best integer equivariant estimator,” *Artificial satellites*, vol. 40, no. 3, pp. 161–171, 2005.
- [19] A. Brack, P. Henkel, and C. Gunther, “Sequential Best Integer-Equivariant Estimation for GNSS,” *Navigation*, vol. 61, no. 2, pp. 149–158, 2014.
- [20] R. Odolinski, P. J. G. Teunissen, and D. Odijk, “Quality analysis of a combined COMPASS/BeiDou-2 and GPS RTK positioning model,” in *IGNSS Symposium*, (Golden Coast, Australia), 16-18 July 2013.
- [21] Y. Yang, J. Li, A. Wang, J. Xu, H. He, H. Guo, J. Shen, and X. Dai, “Preliminary assessment of the navigation and positioning performance of BeiDou regional navigation satellite system,” *Sci. China Earth Sci.*, vol. 57, pp. 144–152, 2014.
- [22] Y. Yang, W. Gao, S. Guo, Y. Mao, and Y. Yang, “Introduction to BeiDou-3 navigation satellite system,” *Navigation*, vol. 66, pp. 7–18, 2019.

- [23] D. Odijk and P. J. G. Teunissen, “Characterization of between-receiver GPS-Galileo inter-system biases and their effect on mixed ambiguity resolution,” *GPS Solut.*, vol. 17, no. 4, pp. 521–533, 2013.
- [24] R. Odolinski and P. J. G. Teunissen, “Low-cost, 4-system, precise GNSS positioning: a GPS, Galileo, BDS and QZSS ionosphere-weighted RTK analysis,” *Meas Sci and Technology*, vol. 28, no. 125801, 2017. doi: 10.1088/1361-6501/aa92eb.
- [25] P. J. G. Teunissen, “Adjustment Theory - An introduction,” *Series on Mathematical Geodesy and Positioning, Faculty of Aerospace Engineering, Delft University of Technology, 2003, The Netherlands*, 2003.
- [26] P. J. G. Teunissen, “An optimality property of the integer least-squares estimator,” *J. Geod.*, vol. 73, pp. 587–593, 1999.
- [27] P. J. G. Teunissen, “The parameter distributions of the integer GPS model,” *J. Geod.*, vol. 76, pp. 41–48, 2002.
- [28] S. Verhagen, “The GNSS integer ambiguities: estimation and validation,” *PhD dissertation, Netherlands Geodetic Commission, Publications on Geodesy, 58*, 2005.
- [29] H. J. Euler and C. Goad, “On optimal filtering of GPS dual frequency observations without using orbit information,” *Bull Geod*, vol. 65, pp. 130–143, 1991.